Finding the best proxies for the solar UV irradiance

Thierry Dudok de Wit, Matthieu Kretzschmar, Jean Lilensten, T. Woods

▶ **To cite this version:**

Thierry Dudok de Wit, Matthieu Kretzschmar, Jean Lilensten, T. Woods. Finding the best proxies for the solar UV irradiance. Geophysical Research Letters, 2009, 36 (10), pp.L10107. 10.1029/2009GL037825 . insu-02770673

HAL Id: insu-02770673

https://insu.hal.science/insu-02770673v1

Submitted on 4 Jun 2020

HAL is a multi-disciplinary open access archive for the deposit and dissemination of scientific research documents, whether they are published or not. The documents may come from teaching and research institutions in France or abroad, or from public or private research centers.

L'archive ouverte pluridisciplinaire **HAL**, est destinée au dépôt et à la diffusion de documents scientifiques de niveau recherche, publiés ou non, émanant des établissements d'enseignement et de recherche français ou étrangers, des laboratoires publics ou privés.

Finding the best proxies for the solar UV irradiance

T. Dudok de Wit,[1] M. Kretzschmar,[1] J. Lilensten,[2] and T. Woods[3]

Received 19 February 2009; revised 30 April 2009; accepted 6 May 2009; published 29 May 2009.

[1] Solar UV emission has a profound impact on the upper terrestrial atmosphere. Because of instrumental constraints, however, solar proxies often need to be used as substitutes for the solar spectral variability. Finding proxies that properly reproduce specific spectral bands or lines is an ongoing problem. Using daily observations from 2003 to 2008 and a multiscale statistical approach, we test the performance of 9 proxies for the UV solar flux. Their relevance is evaluated at different time-scales and a novel representation allows all quantities to be compared simultaneously. This representation reveals which proxies are most appropriate for different spectral bands and for different time scales. **Citation:** Dudok de Wit, T., M. Kretzschmar, J. Lilensten, and T. Woods (2009), Finding the best proxies for the solar UV irradiance, *Geophys. Res. Lett.*, *36*, L10107, doi:10.1029/2009GL037825.

1. Why Are Solar Proxies Needed?

[2] The solar irradiance in wavelengths shortward of 300 nm is a key parameter for the specification of the upper terrestrial atmosphere [*Floyd et al.*, 2002]. Variations are observed on time-scales ranging from seconds to years and can impact radio wave propagation, satellite orbits through increased air-drag but also global Earth climate. Unfortunately, there has been no long-term and continuous measurement of the full solar UV spectrum until Feb. 2002, when the TIMED satellite started operating. Even today, the continuous measurement of solar irradiance with sufficient temporal resolution and radiometric accuracy remains a major instrumental challenge [*Woods et al.*, 2005a]. A important issue is the identification of proper substitutes (i.e., proxies) of the solar UV flux for upper atmospheric modeling [*Lilensten et al.*, 2008].

[3] Here, we test the performance of nine proxies for various UV spectral bands that encompass emissions coming from the solar corona down to the photosphere. The variability should therefore be strongly wavelength dependent, even though different solar layers are coupled. The solar UV radiation mostly affects the terrestrial atmosphere through photoionization and photochemistry, which are again wavelength-dependent processes [*Floyd et al.*, 2002; *Lilensten et al.*, 2008]. The radiation in the MUV range (200–300 nm) mostly affects the stratospheric O_3 concentration; the FUV range (122–200 nm) affects the upper mesospheric O_2 excitation production and the lower thermospheric O_2 dissociation; the EUV range (10–120 nm) affects the thermospheric O, O_2 and N_2 ionization and excitation productions. Other effects include the impact of the intense H I Lyman-α line at 121.57 nm on nitric oxides, which are important for climatological considerations. The altitude of strongest absorption is shown in Figure 1, together with the average spectral irradiance. No single proxy can reproduce the solar variability over the whole UV spectrum. Our prime objective therefore is to compare the measured irradiance in these bands to various proxies that are measured by independent means, partly from ground instruments. Several of these proxies have the advantage of not suffering from instrument degradation and so are easier to maintain in the long.

[4] Many authors have already evaluated the relevance of solar proxies for upper atmosphere specification. Physical models of the solar irradiance [e.g., *Fontenla et al.*, 2007] are not yet accurate enough below 400 nm, so most studies are based on experimental data, using statistical analyses or by comparing specific events [*Parker et al.*, 1998; *Kane*, 2002; *Floyd et al.*, 2005]. Some authors have tested upper atmospheric models with different solar inputs [*Thuillier and Bruinsma*, 2001]. Various empirical models use such proxies to deliver solar UV spectra [*Tobiska et al.*, 2000; *Richards et al.*, 2006].

[5] Our approach is statistical as well. We use daily spectra from the TIMED and SORCE missions, which provide uninterrupted coverage of the full UV spectral range. In contrast to previous studies, however, we first decompose the different quantities into several time-scales before comparing them. Indeed, since different time-scales (e.g., solar rotation period and solar cycle) capture different physical processes, a multiscale approach is needed. The second novelty is a graphical representation, similar to the one used by *Dudok de Wit et al.* [2005], which, for the first time gives a global picture of how all proxies and spectral bands are related to each others, without having to go through the tedious visual comparison of scatter plots or correlation coefficients.

2. Data and Method

[6] We consider daily measurements, covering the declining phase of the solar cycle, from Aug. 2, 2003 until February 1, 2008. Flares are not included here because most instruments don't properly resolve them. The Solar flare [*Tobiska and Bouwer*, 2005] and FISM [*Chamberlin et al.*, 2008] models have been specifically designed to model the short term spectral variability during flares by incorporating high cadence soft X-ray measurements.

[7] Our spectral measurements are a composite of three different instruments. The 1–27 nm and the 121–122 nm ranges are covered by the XPS photometers onboard SORCE [*Woods et al.*, 2005b]. The data (version 9) in that range are not purely observational since the CHIANTI model is used to compute the irradiance in 1 nm bins.

[1] LPC2E, University of Orléans, CNRS, Orléans, France.
[2] LPG, Joseph Fourier University, CNRS, Grenoble, France.
[3] LASP, University of Colorado, Boulder, Colorado, USA.

Copyright 2009 by the American Geophysical Union.
0094-8276/09/2009GL037825

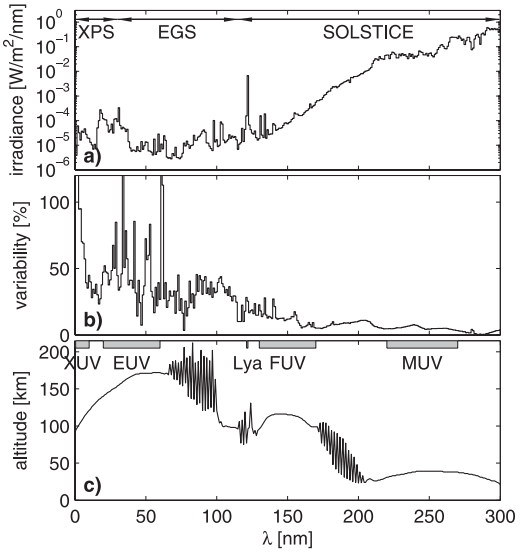

Figure 1. (a) Average solar irradiance for the considered time interval. (b) Variability, defined here as 100× (maximum-minimum)/average irradiance over the period Aug. 2003–Feb. 2008. (c) Altitude of unit optical depth, an indicator of the altitude of maximum atmospheric absorption. The spectral bands refer to the naming conventions used in section 2.

The 27–115 nm range is covered by the EGS spectrograph onboard TIMED [*Woods et al.*, 2005a], whose spectral resolution is 0.4 nm (version 9, the data are rebinned to 1 nm). The remaining wavelengths are covered by the SOLSTICE spectrometers onboard SORCE [*Rottman et al.*, 2006] with a resolution of 1 nm (version 16).

[8] In the following, we concentrate on 5 spectral bands that are considered to be important for aeronomy [*Lilensten et al.*, 2008; *Tobiska et al.*, 2008], see Figure 1. We shall call them XUV (0.5–10 nm), EUV (20–60 nm), Lyman-α (121–122 nm), FUV (130–170 nm) and MUV (220–270 nm). Note that these definitions differ from the ISO 21348:200 standard that was used in section 1. The proxies are:

[9] 1. ISN, the international sunspot number (from SIDC, Brussels), which is not really a UV proxy but remains the most widely used gauge of solar activity.

[10] 2. f10.7 is the radio flux at 10.7 cm (from Penticton Observatory, Canada). This proxy is widely used as a solar input to ionosphere/thermosphere models, partly because it can be conveniently measured from ground.

[11] 3. MgII is the core-to-wing ratio of the Mg II line at 280 nm (from SORCE/SOLSTICE, version 9). This index probes the high chromosphere and is often advocated for the FUV [*Heath and Schlesinger*, 1986].

[12] 4. CaK is the normalized intensity of the Ca II K-line at 393 nm (from National Solar Observatory at Sacramento Peak). This line originates at nearly the same altitude as the Mg II line and has also been advocated for the FUV [*Lean et al.*, 1982].

[13] 5. MPSI is the magnetic plage strength index (from the Mt. Wilson 150-Foot Solar Tower), which quantifies the relative fraction of the solar surface that is covered by mild magnetic fields ($10 < |\mathbf{B}| < 100$ Gauss). By definition, the MPSI index is a proxy for plages and faculae [*Parker et al.*, 1998].

[14] 6. MWSI is the Mount Wilson sunspot index, defined as the MPSI, but for intense magnetic fields ($|\mathbf{B}| > 100$ Gauss). The MWSI is a proxy for active regions.

[15] 7. s10.7 is computed by *Tobiska et al.* [2008] out of the integrated 26–34 nm emission from the SEM radiometer onboard SoHO, and rescaled to the f10.7 index after a trend correction (version 3.9a). This proxy is dominated by the emission from the chromospheric and transition region He II line at 30.4 nm.

[16] 8. Lyman-α channel (ch-L) is the expected output of a photodiode from the LYRA radiometer [*Hochedez et al.*, 2006] onboard the PROBA2 satellite, whose launch is scheduled for the end of 2009. This channel integrates emissions in the 110–210 nm band, with a peak around 125 nm. We reconstructed the signal from SORCE/SOLSTICE data.

[17] 9. Herzberg channel (ch-H) is the expected output of a photodiode from LYRA in the Herzberg band, here between 195–220 nm. Both the Herzberg and the Lyman-α channels are relevant inputs for upper atmospheric models.

[18] Note that the last three quantities are actually derived from UV irradiance measurements and so do not really qualify as proxies. Together with the MgII index, they must be measured from space.

[19] To compare different time-scales, we first decompose each quantity into different scales using the *à trous* wavelet decomposition [*Mallat*, 1998]. The decomposition imposes scales that are centered on 3, 6, 12, 24,..., 768 days. The components associated with scales of 24 and 96 days are illustrated in Figure 2. The first scale captures solar rotation effects and the second one the long-term evolution of active regions. The most conspicuous result in Figure 2 is the remarkable coherence of all quantities, which justifies *a posteriori* the widespread use of proxies for the solar UV flux.

[20] All quantities are affected by various types of noise. The signal-to-noise ratio of the irradiance degrades as the flux drops with decreasing solar cycle and detector degradation increases. Data gaps in the CaK (with 22% coverage

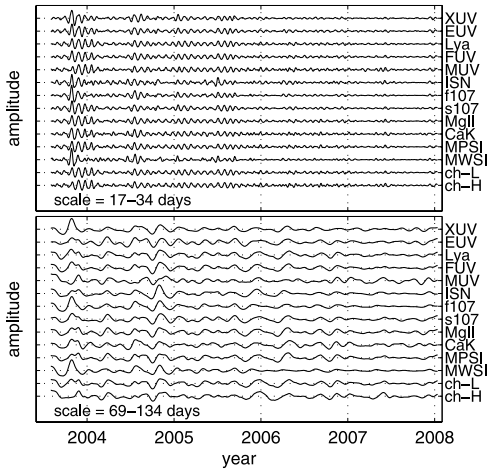

Figure 2. Decomposition of the 5 spectral bands and the 9 proxies into two different scales: (top) solar rotation period and (bottom) an average time-scale of 96 days. Amplitudes are arbitrary. The legends are given in the text.

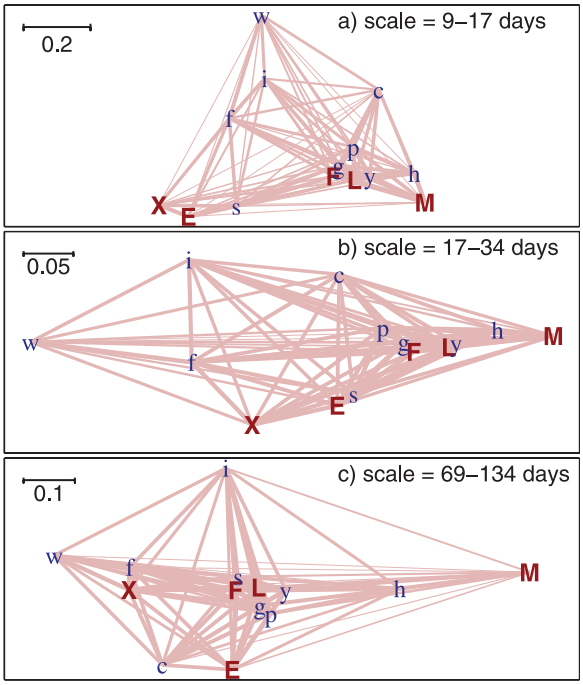

Figure 3. Correspondence maps for three characteristic scales. The distance between each pair of points corresponds to $1 - |r|$ (see text) and the line thickness is proportional to r. Capitals designate our 5 spectral bands: (X)UV, (E)UV, H I (L)yman-α, (F)UV and (M)UV. The other characters correspond to proxies: (i)sn, (f)10.7, (s)10.7, M(g)II, (c)aK, M(p)SI, M(w)SI, L(y)man-α channel, (h)erzberg channel.

and a median gap duration of 3 days), MPSI and MWSI (75% coverage, 1 day median) indices were filled by multivariate interpolation [*Kondrashov and Ghil*, 2006]. Gap filling affects the variability on the shortest time-scales (up to about 6 days) by enhancing the correlation with other proxies. The smallest scales require more careful analysis and are therefore discarded here.

3. Proxy-to-Spectral Band Relation

[21] Since all quantities are strongly correlated, we use the Pearson correlation coefficient $r_{xy} = s_{xy}/(s_x s_y)$ (where s_{xy} is the sample covariance, and s_x^2 is the sample variance) as a gauge of linear correspondence between x and y. Unfortunately, this quantity can only be computed pairwise, leaving us with a large table of values to decipher. Better insight can be gained by turning these values into a graph, using the multidimensional scaling technique [*Borg and Groenen*, 1997]. The idea consists in representing all irradiances and proxies on a 2D correspondence map in such a way that their mutual distance equals their dissimilarity, defined here as $d = 1 - |r|$. Such a map allows the proxy-to-spectral band relation to be investigated in detail. Two close variants of this approach have already been used by *Dudok de Wit et al.* [2005, 2008].

[22] In principle, we would need a 13-dimensional plot to represent all quantities while accounting for their mutual distances exactly [*Borg and Groenen*, 1997]. However, because of the strong coherency of the spectral variability, a 2D (and sometimes even a 1D) approximation already captures the salient statistical features. We verified that a third dimension does not bring new insight here.

[23] Figure 3 is the central result of this study, as it shows the correspondence between proxies and spectral bands for three typical scales. What matters in these plots is the distance between each pair, and not the absolute positions or the axes, which do not carry any direct meaning. The closer two quantities are, the more correlated they are. The correspondence map therefore provides both quantitative (the distance is related to r) and qualitative information on how all quantities are related to each other. Figure 3a covers time-scales of typically half a solar rotation, Figure 3b one solar rotation and Figure 3c several rotations. It comes as no surprise that quantities with strong physical connections, such as the Lyman-α band and the Lyman-α channel, always stick together.

[24] Interestingly, all spectral bands are roughly distributed along a line, revealing a gradual transition from optically thin and energetic emissions on the left to optically thick ones on the right. For time-scales below one solar rotation (upper plot), this ordering manifests itself in the center-to-limb variation, with brightenings in the XUV and EUV bands, and darkenings in the FUV and MUV bands [*Donnelly and Puga*, 1990]. Our maps show that the same gradual transition persists for longer time-scales. The relative location of proxies with respect to this alignment changes substantially with time-scale, which confirms and highlights the importance of a multiscale approach.

[25] Figure 3c focuses on time-scales that encompass the decay time of active regions. Similar distributions are observed for larger scales but the solar cycle time scale could not be addressed by lack of data. Some correlations are difficult to explain, such as the close location of the MgII index and the EUV band, already noted by *Judge et al.* [2002]. Equally surprising is the difference between the MgII and CaK indices, which probe nearly the same solar altitude.

4. Conclusions and Recommendations

[26] What are the best proxies for reconstructing specific spectral bands? Figure 3 precisely tells us that the answer very much depends on the time-scale of interest. Several general conclusions can nevertheless be drawn.

[27] 1. Proxies that are derived from real irradiance data do indeed match their corresponding spectral band quite well. The correlation between the LYRA Lyman-α channel and the Lyman-α band, for example, always exceeds 0.95.

[28] 2. The MgII index shows the best global performance since it is always located close to the center of the cloud of points. It is particularly well suited for the FUV band. The MPSI index is a backup solution, but is not measured continuously.

[29] 3. Apart from these, however, no single spectral band can be properly reconstructed at all scales from one single proxy.

[30] 4. There is no good (non irradiance-derived) proxy for the XUV and EUV bands. The f10.7 index would be the least bad solution.

[31] 5. None of our proxies properly fits the MUV band, for which a better gauge of photospheric emissions is needed.

[32] The correspondence map can also be used to search for new proxies. Indeed, when three quantities are closely spaced and aligned, then the one in the middle can be approximated by taking a linear combination of the two others. Two spectral bands whose reconstruction can be improved that way are the FUV and the Lyman-α bands. Reciprocally, remotely located quantities are hardest to reconstruct. This is particularly evident for the MUV and the XUV bands. For the same reason, the sunspot number and the MWSI should not be used for any reconstruction as they capture variations that are not reproduced by the irradiance.

[33] We are currently developing this multiscale approach for more accurate reconstructions of the previously considered UV bands. The EUV band, for example, can be reconstructed as a sum of contributions from different proxies, decomposed into different scales and with different weights. Our tests show that the residual error between the observed and modeled flux can be reduced that way by a factor of 2 to 4 as compared to models that do not consider multiple scales. These results will be detailed in a forthcoming publication. A second improvement consists in incorporating the effect of a convolution with time, as studied by *Preminger and Walton* [2007]. An aspect that matters for operational models is the availability of the proxies, since their long-term measurement is not always guaranteed.

[34] **Acknowledgments.** We thank two anonymous referees for their helpful comments. The following institutes are acknowledged for providing the data: Solar Influences Data Center (Brussels), Laboratory for Atmospheric and Space Physics (Boulder), National Geophysical Data Center (NOAA), National Solar Observatory at Sacramento Peak (data produced cooperatively by NSF/NOAO, NASA/GSFC and NOAA/SEC) and Mount Wilson Observatory (operated by UCLA, with funding from NASA, ONR and NSF, under agreement with the Mt. Wilson Institute). Thanks are also due to K. Tobiska (Space Environment Technologies) for providing the s10.7 index and I. Dammasch (SIDC) for providing the passbands of LYRA. This study received funding from the French PNST programme and from the European Community's Seventh Framework Programme (FP7/2007-2013) under the grant agreement 218816 (SOTERIA project, www.soteria-space.eu).

References

Borg, I., and P. Groenen (1997), *Modern Multidimensional Scaling: Theory and Applications*, Springer, Berlin.

Chamberlin, P. C., T. N. Woods, and F. G. Eparvier (2008), New flare model using recent measurements of the solar ultraviolet irradiance, *Adv. Space Res.*, *42*, 912–916, doi:10.1016/j.asr.2007.09.009.

Donnelly, R. F., and L. C. Puga (1990), Thirteen-day periodicity and the center-to-limb dependence of UV, EUV, and X-ray emission of solar activity, *Sol. Phys.*, *130*, 369–390.

Dudok de Wit, T., J. Lilensten, J. Aboudarham, P.-O. Amblard, and M. Kretzschmar (2005), Retrieving the solar EUV spectrum from a reduced set of spectral lines, *Ann. Geophys.*, *23*, 3055–3069.

Dudok de Wit, T., M. Kretzschmar, J. Aboudarham, P.-O. Amblard, F. Auchère, and J. Lilensten (2008), Which solar EUV indices are best for reconstructing the solar EUV irradiance?, *Adv. Space Res.*, *42*, 903–911, doi:10.1016/j.asr.2007.04.019.

Floyd, L., W. K. Tobiska, and R. P. Cebula (2002), Solar UV irradiance, its variation, and its relevance to the Earth, *Adv. Space Res.*, *29*, 1427–1440.

Floyd, L., J. Newmark, J. Cook, L. Herring, and D. McMullin (2005), Solar EUV and UV spectral irradiances and solar indices, *J. Atmos. Sol. Terr. Phys.*, *67*, 3–15, doi:10.1016/j.jastp.2004.07.013.

Fontenla, J. M., K. S. Balasubramaniam, and J. Harder (2007), Semiempirical models of the solar atmosphere. II. The quiet-Sun low chromosphere at moderate resolution, *Astrophys. J.*, *667*, 1243–1257, doi:10.1086/520319.

Heath, D. F., and B. M. Schlesinger (1986), The Mg 280-nm doublet as a monitor of changes in solar ultraviolet irradiance, *J. Geophys. Res.*, *91*, 8672–8682.

Hochedez, J.-F., et al. (2006), LYRA, a solar UV radiometer on Proba2, *Adv. Space Res.*, *37*, 303–312, doi:10.1016/j.asr.2005.10.041.

Judge, D. L., H. S. Ogawa, D. R. McMullin, P. Gangopadhyay, and J. M. Pap (2002), The SOHO CELIAS/SEM EUV database from SC23 minimum to the present, *Adv. Space Res.*, *29*, 1963–1968.

Kane, R. P. (2002), Correlation of solar indices with solar EUV fluxes, *Sol. Phys.*, *207*, 17–40.

Kondrashov, D., and M. Ghil (2006), Spatio-temporal filling of missing points in geophysical data sets, *Nonlinear Processes Geophys.*, *13*, 151–159.

Lean, J. L., O. R. White, W. C. Livingston, D. F. Heath, R. F. Donnelly, and A. Skumanich (1982), A three-component model of the variability of the solar ultraviolet flux: 145–200 nM, *J. Geophys. Res.*, *87*, 10,307–10,317.

Lilensten, J., T. Dudok de Wit, M. Kretzschmar, P.-O. Amblard, S. Moussaoui, J. Aboudarham, and F. Auchère (2008), Review on the solar spectral variability in the EUV for space weather purposes, *Ann. Geophys.*, *26*, 269–279.

Mallat, S. (1998), *A Wavelet Tour of Signal Processing*, Academic, San Diego, Calif.

Parker, D. G., R. K. Ulrich, and J. M. Pap (1998), Modeling solar UV variations using Mount Wilson Observatory indices, *Sol. Phys.*, *177*, 229–241.

Preminger, D. G., and S. R. Walton (2007), From sunspot area to solar variability: A linear transformation, *Sol. Phys.*, *240*, 17–23, doi:10.1007/s11207-007-0335-2.

Richards, P. G., T. N. Woods, and W. K. Peterson (2006), HEUVAC: A new high resolution solar EUV proxy model, *Adv. Space Res.*, *37*, 315–322, doi:10.1016/j.asr.2005.06.031.

Rottman, G. J., T. N. Woods, and W. McClintock (2006), SORCE solar UV irradiance results, *Adv. Space Res.*, *37*, 201–208, doi:10.1016/j.asr.2005.02.072.

Thuillier, G., and S. Bruinsma (2001), The Mg II index for upper atmosphere modelling, *Ann. Geophys.*, *19*, 219–228.

Tobiska, W., and S. Bouwer (2005), Solar flare evolution model for operational users, in *Ionospheric Effects Symposium*, edited by J. M. Goodman, pp. 1–6, Off. of Nav. Res., Washington, D. C.

Tobiska, W. K., T. Woods, F. Eparvier, R. Viereck, L. Floyd, D. Bouwer, G. Rottman, and O. R. White (2000), The SOLAR2000 empirical solar irradiance model and forecast tool, *J. Atmos. Sol. Terr. Phys.*, *62*, 1233–1250.

Tobiska, W., S. Bouwer, and B. Bowman (2008), The development of new solar indices for use in thermospheric density modeling, *J. Atmos. Sol. Terr. Phys.*, *70*, 803–819, doi:10.1016/j.jastp.2007.11.001.

Woods, T. N., F. G. Eparvier, S. M. Bailey, P. C. Chamberlin, J. Lean, G. J. Rottman, S. C. Solomon, W. K. Tobiska, and D. L. Woodraska (2005a), Solar EUV Experiment (SEE): Mission overview and first results, *J. Geophys. Res.*, *110*, A01312, doi:10.1029/2004JA010765.

Woods, T. N., G. J. Rottman, and R. Vest (2005b), XUV Photometer System (XPS): Overview and calibrations, *Sol. Phys.*, *230*, 345–374, doi:10.1007/s11207-005-4119-2.

T. Dudok de Wit and M. Kretzschmar, LPC2E, 3A av. de la Recherche Scientifique, F-45071 Orléans CEDEX, France. (ddwit@cnrs-orleans.fr; matthieu.kretzschmar@cnrs-orleans.fr)

J. Lilensten, LPG, BP 53, F-38041 Grenoble CEDEX, France. (jean.lilensten@obs.ujf-grenoble.fr)

T. Woods, LASP, University of Colorado, 1234 Innovation Drive, Boulder, CO 80303, USA. (tom.woods@lasp.colorado.edu)